

# Inverted type bulk-heterojunction organic solar cell using electrodeposited titanium oxide thin films as electron collector electrode

メタデータ	言語: eng 出版者: 公開日: 2017-10-03 キーワード (Ja): キーワード (En): 作成者: メールアドレス: 所属:
URL	<a href="https://doi.org/10.24517/00010929">https://doi.org/10.24517/00010929</a>

This work is licensed under a Creative Commons Attribution-NonCommercial-ShareAlike 3.0 International License.



Inverted type bulk-heterojunction organic solar cell using electrodeposited titanium oxide thin films as electron collector electrode

Takayuki Kuwabara\*, Hirokazu Sugiyama, Takahiro Yamaguchi, Kohshin Takahashi\*

Graduate School of Natural Science and Technology, Kanazawa University, Kakuma-machi,  
Kanazawa, Ishikawa 920-1192, Japan

\* Corresponding author: TEL: +81-76-234-4770  
FAX: +81-76-234-4800  
E-mail: [tkuwa@t.kanazawa-u.ac.jp](mailto:tkuwa@t.kanazawa-u.ac.jp)

Submitted to *Thin Solid Films*

## **Abstract**

We developed an inverted type bulk-heterojunction organic solar cell with 1 cm<sup>2</sup> active area using a fluorine-doped tin oxide / electrodeposited amorphous (TiO<sub>x</sub>) or anatase (TiO<sub>2</sub>) titanium oxide electrode instead of the low work-functional electrode such as Al. The cell with TiO<sub>2</sub> showed the power conversion efficiency ( $\eta$ ) of 2.5 % by irradiating AM 1.5-100 mW cm<sup>-2</sup> simulated sunlight. While, the performance of the cell with TiO<sub>x</sub> was almost maintained in an ambient atmosphere under continuous light irradiation of 10 h, although slightly small initial  $\eta$  value of 2.1% was observed.

Key words: Organic thin film solar cells, electrodeposited titanium oxide, air-stable

## Main Text

### 1. Introduction

Organic solar cells have been attracting much attention as a candidate for socially acceptable “renewable energy source” instead of the fossil fuel due to providing lower cost and environment-friendly energy conversion system. An Al metal has been often used as the anodic electrode of the organic solar cells, which are termed “normal type solar cells” as shown in Figure 1(a), because of its low work function. But there is a problem for its durability because the Al surface is easily oxidized to insulator  $\text{Al}_2\text{O}_3$  in air. Recently, the developments of the solar cells using non-corrosive electrode instead of the Al anode have been carried out by several research groups in order to solve this problem. Their solar cells have the inverted device structure against normal type solar cells, that is, their photo-generated electrons flow through external circuit from the ITO electrode to Au electrode. Therefore they are called “inverted type solar cells” as shown in Figure 1(b). Although metals such as In [1-3] or n-type semiconductors such as  $\text{TiO}_2$  [4-8] and ZnO [3, 9, 10] prepared by a sol-gel technique have been often used as electron collector electrodes of the inverted type solar cells, the organic thin film solar cells using an electrodeposited technique have hardly been developed. Because the fabrication of the solar cells requires the control of each layer in nanometer-scale thickness, it is not tried to apply the electrodeposited film having an unevenness surface for the solar cells. In our research, we developed the inverted type solar cells using the electrodeposited amorphous ( $\text{TiO}_x$ ) and anatase titanium oxide ( $\text{TiO}_2$ ) layers. Figure 1(c) shows the energy-level diagram of the inverted type solar cells. n-Type transparent semiconductor  $\text{TiO}_x$  and  $\text{TiO}_2$  layers were expected as an electron collector because the bottom energy level of the conduction band of titanium(IV) oxide located down to the LUMO level of acceptor PCBM. Herein, we report the performance of a

fluorine-doped tin oxide (FTO)/TiO<sub>x</sub> or TiO<sub>2</sub>/regioregular poly(3-hexylthiophene) (P3HT):[6,6]-phenyl C<sub>61</sub> butyric acid methyl ester (PCBM)/poly(3,4-ethylenedioxyethiophene):poly(4-styrene sulfonic acid) (PEDOT:PSS)/Au inverted type bulk-heterojunction organic solar cell.

## **2. Experiments**

### **2.1. Materials.**

Titanium(IV) oxysulfate solution (TiOSO<sub>4</sub>, 99.99 %, ~15 wt. % in dilute sulfuric acid), titanium(IV) isopropoxide (Ti[OCH(CH<sub>3</sub>)<sub>2</sub>]<sub>4</sub>, 99.999 %), 2-methoxyethanol (CH<sub>3</sub>OCH<sub>2</sub>CH<sub>2</sub>OH, 99.9 %), acetyl acetone (AA; CH<sub>3</sub>C(O)CH<sub>2</sub>C(O)CH<sub>3</sub>, 99 %), regioregular P3HT (M<sub>w</sub> ~ 87,000), PEDOT-PSS 1.3 wt% dispersion in water, and chlorobenzene were purchased from Sigma-Aldrich Chemical Co., Inc. Hydrogen peroxide (H<sub>2</sub>O<sub>2</sub>, 30.0 ~ 35.5 %) and 2-propanol (dehydrated, 99.5 %) were purchased from Kanto Chemical Co., Inc. All the chemicals were used as received. FTO substrate (A110U80, 12 Ω/□) was purchased from AGC Fabritech Co., Ltd.

### **2.2. Fabrications of organic thin film solar cells using electrodeposited titanium oxide thin films.**

All the operations except the vacuum deposition and the sealing treatment were implemented in air. An FTO electrode was used as transparent conductive oxide, because its electric resistance hardly increased by heat treatment at 450 °C and it has a resistance to electrochemical reduction. The FTO electrode was ultrasonicated in 2-propanol, and then cleaned in boiling 2-propanol, and subsequently dried. The titanium oxide precursor (TiO(OH)<sub>2</sub> · x H<sub>2</sub>O) film was prepared on the FTO by electrodepositing potentiostatically at -2.2 V vs Ag/AgCl in a solution containing 0.01 M TiOSO<sub>4</sub>, 0.03 M H<sub>2</sub>O<sub>2</sub>, and 0.3 M KNO<sub>3</sub>

[11, 12] and by consuming the electric charge of  $400 \text{ mC cm}^{-2}$ . After the as-deposited film was washed with water and dried in air, the  $\text{TiO}(\text{OH})_2 \cdot x \text{ H}_2\text{O}$  was converted to the amorphous  $\text{TiO}_x$  or the crystalline  $\text{TiO}_2$  by heat treatment at 150 or 450 °C for 1 h. The preparation of sol-gel  $\text{TiO}_x$  precursor film was based on the method described by Kim et al[13, 14]. Titanium (IV) isopropoxide (2.4 g, 8.44 mmol) was slowly added to 2-methoxyethanol (12.5 mL) cooled by an ice bath to avoid drastic temperature increase, and then the mixture solution was refluxed for 1 h. Further, the solution was cooled by the ice bath, and AA (2.07 g, 20.7 mmol) as the stabilizer was slowly added to its cooled solution, followed by refluxing for 1 h to obtain the  $\text{TiO}_x$  precursor solution. AA- $\text{TiO}_x$  precursor solutions took on yellow. The precursor solution was spin-coated at 2000 rpm on FTO being accompanied by hydrolysis in an ambient atmosphere and by heat treatment at 150 °C for 1 h. A sol-gel anatase  $\text{TiO}_2$  film was prepared by heating a  $\text{TiO}_x$  precursor coated FTO electrode at 450 °C for 30 min. A bulk-heterojunction active layer was prepared onto the as-prepared FTO/ $\text{TiO}_x$  or  $\text{TiO}_2$  substrate by spin-coating at 700 rpm a mixed chlorobenzene solution containing  $25 \text{ g L}^{-1}$  P3HT and  $20 \text{ g L}^{-1}$  PCBM. Further, a PEDOT:PSS aqueous dispersion solution was spin-coated at 6000 rpm onto its blend film. Finally, an Au metal as the back cathode was vacuum-deposited on the PEDOT:PSS solid film, the effective area of the solar cell being restricted to  $1.0 \text{ cm}^2$  by a shadow mask. The device was heated at 150 °C for an annealing treatment. If necessary, the device was covered with a glass plate coated by an epoxy UV resin as sealing material in an  $\text{N}_2$  filled glove box. After charging a water getter sheet (Komatsu Seiren Co., Ltd.) into the slight space of about  $40 \text{ }\mu\text{m}$  thickness between the device surface and the glass plate, the sealing treatment was finally completed by irradiating UV light to the epoxy resin.

### **2.3. Measurement.**

The X-ray diffraction (XRD) measurement was carried out using an X-ray diffractometer Rigaku RINT 2500 with Cu K $\alpha$  radiation at 20 kV x 10 mA. A Hitachi S-4500 scanning electron microscopic (SEM) operated at an accelerating voltage of 15 kV was used in order to observe the surface morphology of the titanium oxide and estimate the thickness of each layer in the device. The photocurrent-voltage (I-V) curves of the solar cells were measured at 5 V min<sup>-1</sup> of a scan rate in linear sweep voltammetry (LSV) under a solar simulated light AM 1.5-100 mW cm<sup>-2</sup> by a Kansai Kagakukikai XES-502S solar simulator. Durability test of the solar cells was carried out by an interval LSV measurement in combination with a rest voltage measurement under continuous irradiation of the AM1.5-100 mW cm<sup>-2</sup> light. All the electric measurements were implemented in an ambient atmosphere using a Hokuto Denko HZ-5000 electrochemical analyzer. Ionization potentials for P3HT, PCBM, PEDOT:PSS, FTO, and Au were estimated by a Riken Keiki model AC-2, and band gap energies for P3HT and PCBM by a Hitachi U-3310 spectrophotometer.

### 3. Results and Discussion

The XRD pattern of the electrodeposited titanium oxide film on the FTO electrode after heating at 450 °C showed two peaks at  $2\theta = 25.2^\circ$  and  $2\theta = 48^\circ$  labeled orientation along the (101) and (200) planes, respectively. This TiO<sub>2</sub> was assigned to an anatase-type crystal structure. In contrast, the XRD pattern of the film after heating at 150 °C showed no peaks, indicating that the titanium oxide is an amorphous TiO<sub>x</sub>. Surface SEM images of the TiO<sub>x</sub> and TiO<sub>2</sub> films are shown in Figure 2. The SEM images showed that the both FTO substrates are densely covered with titanium oxide particles of ca. 20 ~ 50 nm size. Cross sectional SEM images of the electrodeposited film and the sol-gel prepared film are shown in Figures 2(d) and (e). Although the electrodeposited film was more irregular than the sol-gel prepared film, thicknesses of both films were ca. 90-100 nm.

Figure 3 shows the photo I-V curves of the inverted type solar cells with and without titanium oxide layers. The performance of the cell without the layer showed the short-circuit photocurrent ( $J_{sc}$ ) of  $5.28 \text{ mA cm}^{-2}$ , the open-circuit voltage ( $V_{oc}$ ) of  $0.32 \text{ V}$ , the fill factor (FF) of  $0.26$ , and the power conversion efficiency ( $\eta$ ) of  $0.45 \%$ , see curve (a). Whereas, the performance of the cell with electrodeposited amorphous  $\text{TiO}_x$  layer showed  $J_{sc} = 6.95 \text{ mA cm}^{-2}$ ,  $V_{oc} = 0.55 \text{ V}$ ,  $\text{FF} = 0.56$ , and  $\eta = 2.13 \%$ , see curve (b), the  $\eta$  value being 4.7 times higher than that without the  $\text{TiO}_x$  layer. This result implies that the rectification property of the device was improved because the  $\text{TiO}_x$  layer acted as both of electron-collecting and hole-blocking layers. That is, when the electrodeposited  $\text{TiO}_x$  layer covered almost completely on the FTO substrates, the recombination between the collected electrons into the n-type semiconductor  $\text{TiO}_x$  and the resided holes in P3HT:PCBM blend was remarkably suppressed. Additionally, the  $\eta$  value of the cell with the electrodeposited anatase  $\text{TiO}_2$  layer increased up to  $2.48 \%$  by the improvement of  $J_{sc}$  ( $7.88 \text{ mA cm}^{-2}$ ), see curve (c). This suggests that the carrier density and/or the electron mobility in the  $\text{TiO}_2$  layer increased with a crystallization of the titanium oxide layer by the heat treatment. However, in the control experiment employing the  $\text{TiO}_2$  layer prepared by sol-gel technique, the solar cell showed  $\eta$  of  $1.99 \%$ , see curve (d). This FTO surface has a texture structure to gain the photocurrent quantum yield by light scattering, being composed of mountains of about  $200 \text{ nm}$  height with the width of  $100 \sim 300 \text{ nm}$  as shown in Figure 2 (a). Therefore, the  $\text{TiO}_2$  layer was partially very thin although it covered roughly on the FTO substrates by the sol-gel method, see Figure 2 (e). The recombination between the collected electrons in  $\text{TiO}_2$  and the resided holes in P3HT:PCBM blend may occur partly at the interface of the thin  $\text{TiO}_2$  layer.

In the time course of the photo I-V curves of the solar cells with the electrodeposited  $\text{TiO}_x$  and  $\text{TiO}_2$  films, when the anatase  $\text{TiO}_2$  layer was inserted between the FTO substrate and the P3HT:PCBM organic layer, the  $\eta$  reached the maximum value within a few minutes

after light irradiation. In contrast, for the cell with the amorphous  $\text{TiO}_x$ , the improvement of the cell performance was observed very slowly with increasing the irradiation time. As a result, the maximum performance was obtained after irradiating for 90 min. The difference of its time dependence implies that the carrier density in the  $\text{TiO}_x$  is lower than that in the  $\text{TiO}_2$ , reflecting that the  $J_{sc}$  value of the cell with  $\text{TiO}_2$  was larger than that with  $\text{TiO}_x$  as shown in Figure 3.

The photo I-V curves of the FTO/electrodeposited amorphous  $\text{TiO}_x$ /P3HT:PCBM/PEDOT:PSS/Au and the FTO/electrodeposited anatase  $\text{TiO}_2$ /P3HT:PCBM/PEDOT:PSS/Au inverted type solar cells were measured with and without a UV light cut filter which takes off the light of less than 440 nm being slightly contained in AM1.5-100  $\text{mW cm}^{-2}$  simulated sunlight, see Figure 4. For the  $\text{TiO}_x$  inserted cell, the photocurrent was not absolutely observed by the light irradiation with the filter, see curve (a). But the  $\eta$  of 2.13 % was obtained by the irradiation without the filter, see curve (c). On the other hand, when the anatase  $\text{TiO}_2$  cell ( $\eta = 2.48$  %) was covered by the filter, the performance decreased down to 0.39 %, see curve (b). The electrons produced in the  $\text{TiO}_x$  and  $\text{TiO}_2$  bulk by irradiating UV light may fill firstly into electron traps of the titanium oxide interfering with the electron transport, and secondly after irradiating the UV light for a short period of time, they may transport relatively smooth because of the decrease of the trap sites.

The durability test was carried out in an ambient atmosphere. The comparison of the  $\eta$  against irradiation time for the inverted type organic solar cells with an amorphous  $\text{TiO}_x$  (open square) and an anatase  $\text{TiO}_2$  (open circle) is shown in Figure 5. For the  $\text{TiO}_2$  inserted type solar cell, the  $\eta$  decreased down to 80 % of the maximum value after light irradiation for 10 h, probably because of a photo-catalytic effect by anatase  $\text{TiO}_2$ . In contrast, the  $\eta$  for the solar cell with the  $\text{TiO}_x$  layer was almost maintained under continuous light irradiation for 10 h. Furthermore, when this cell with the  $\text{TiO}_x$  layer was sealed using a glass plate, the

performance maintained 85 % of the maximum  $\eta$  value even after continuous light irradiation for 100 h. (Not shown) I believe that the stability of our cell is extremely high.

#### **4. Conclusions**

The present paper is report for the development and the performance evaluation of the inverted type organic solar cells inserting an electrodeposited titanium oxide layer between the FTO substrate and the P3HT:PCBM blend layer.

The  $\eta$  values of 2.1 and 2.5 % were obtained for the inverted type organic solar cells with the amorphous  $\text{TiO}_x$  and the anatase  $\text{TiO}_2$ , respectively. The  $\text{TiO}_x$  device without sealing exposed to air showed the high durability under continuous irradiation of AM 1.5-100  $\text{mW cm}^{-2}$  simulated sunlight for 10 h. In addition, this device with sealing maintained the relative efficiency over 85 % under continuous light irradiation for 100 h in air. These imply that the amorphous  $\text{TiO}_x$  and  $\text{TiO}_2$  play an important role as both of the electron collection layer and the hole blocking layer, and inserting amorphous  $\text{TiO}_x$  is effective for preventing the performance degradation under continuous light irradiation. It will be possible to make more efficient and air-stable solar cells by controlling the surface morphology and the electric resistance of  $\text{TiO}_x$  and  $\text{TiO}_2$ .

#### **Acknowledgements**

This work was supported by the Incorporated Administrative Agency New Energy and Industrial Technology Development Organization (NEDO) under Ministry of Economy, Trade and Industry (METI).

#### **References**

- [1] J.-i. Nakamura, C. Yokoe, K. Murata, K. Takahashi, *J. Appl. Phys.* 96 (2004) 6878-6883.
- [2] J.-i. Nakamura, S. Suzuki, K. Takahashi, C. Yokoe, K. Murata, *Bull. Chem. Soc. Jpn.* 77 (2004) 2185-2188.
- [3] K. Takahashi, T. Nishi, S. Suzaka, Y. Sigeyama, T. Yamaguchi, J.-i. Nakamura, K. Murata, *Chem. Lett.* 34 (2005) 768-769.
- [4] C. Waldauf, M. Morana, P. Denk, P. Schilinsky, K. Coakley, S. A. Choulis, C. J. Brabec, *Appl. Phys. Lett.* 89 (2006) 233517-1-3.
- [5] R. Steim, S. A. Choulis, P. Schilinsky, C. J. Brabec, *Appl. Phys. Lett.* 92 (2008) 093303-1-3.
- [6] G. K. Mor, K. Shankar, M. Paulose, O. K. Varghese, C. A. Grimes, *Appl. Phys. Lett.* 91 (2007) 152111-1-3.
- [7] K. Takahashi, K. Seto, T. Yamaguchi, J.-i. Nakamura, C. Yokoe, K. Murata, *Chem. Lett.* 33 (2004) 1042-1043.
- [8] K. Takahashi, T. Nakanishi, T. Yamaguchi, J.-i. Nakamura, K. Murata, *Chem. Lett.* 34 (2005) 714-715.
- [9] D. C. Olson, J. Pirus, R. T. Collins, S. E. Shaheen, D. S. Ginley, *Thin Solid Films* 496 (2006) 26-29.
- [10] K. Takanezawa, K. Hirota, Q.-S. Wei, K. Tajima, K. Hashimoto, *J. Phys. Chem. C* 111 (2007) 7218-7223.
- [11] C. Natarajan, G. Nogami, *Journal of The Electrochemical Society* 143 (1996) 1547-1550.
- [12] S. Karuppuchamy, K. Nonomura, T. Yoshida, T. Sugiura, H. Minoura, *Solid State Ionics* 151 (2002) 19-27.

- [13] J. Y. Kim, S. H. Kim, H.-H. Lee, K. Lee, W. Ma, X. Gong, A. J. Heeger, *Adv. Mater.* 18 (2006) 572-576.
- [14] J. Y. Kim, K. Lee, N. E. Coates, D. Moses, T.-Q. Nguyen, M. Dante, A. J. Heeger, *Science* 317 (2007) 222-225.

## Figure captions

Figure 1 Schematic structures of a normal (a) and an inverted type organic solar cells (b), and energy-level diagram (c) showing the work functions and the HOMO-LUMO energies of the component materials.

Figure 2 Surface SEM images of the bare FTO substrate (a), the as-synthesized  $\text{TiO}_x$  (b) and  $\text{TiO}_2$  films (c) obtained from annealing the electrodeposited films at 150 °C and 450 °C, respectively. Cross sectional SEM images of the electrodeposited  $\text{TiO}_2$  film (d) and the sol-gel prepared  $\text{TiO}_2$  film (e) on the FTO substrates.

Figure 3 Photo I-V curves of the solar cells without the  $\text{TiO}_2$  layer (a) and with the electrodeposited amorphous  $\text{TiO}_x$  layer (b), the electrodeposited anatase  $\text{TiO}_2$  layer (c), and the  $\text{TiO}_2$  layer prepared by a sol gel method (d), respectively.

Figure 4 Photo I-V curves of the FTO/amorphous  $\text{TiO}_x$ /P3HT:PCBM/PEDOT:PSS/Au and FTO/anatase  $\text{TiO}_2$ /P3HT:PCBM/PEDOT:PSS/Au type solar cells under light irradiation of AM 1.5-100  $\text{mW cm}^{-2}$  with and without UV light cut filter ( $< 440 \text{ nm}$ ).

Figure 5 Irradiation time dependences of the  $\eta$  for the inverted type organic solar cells with an amorphous  $\text{TiO}_x$  layer (open square) and an anatase  $\text{TiO}_2$  layer (open circle).

The cells were exposed in air during the irradiation.

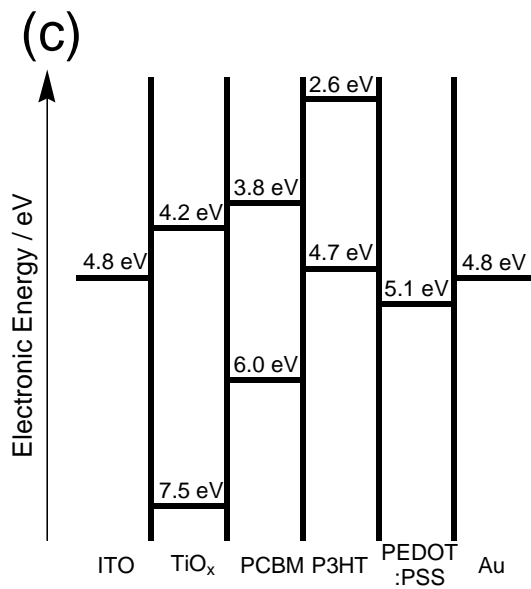
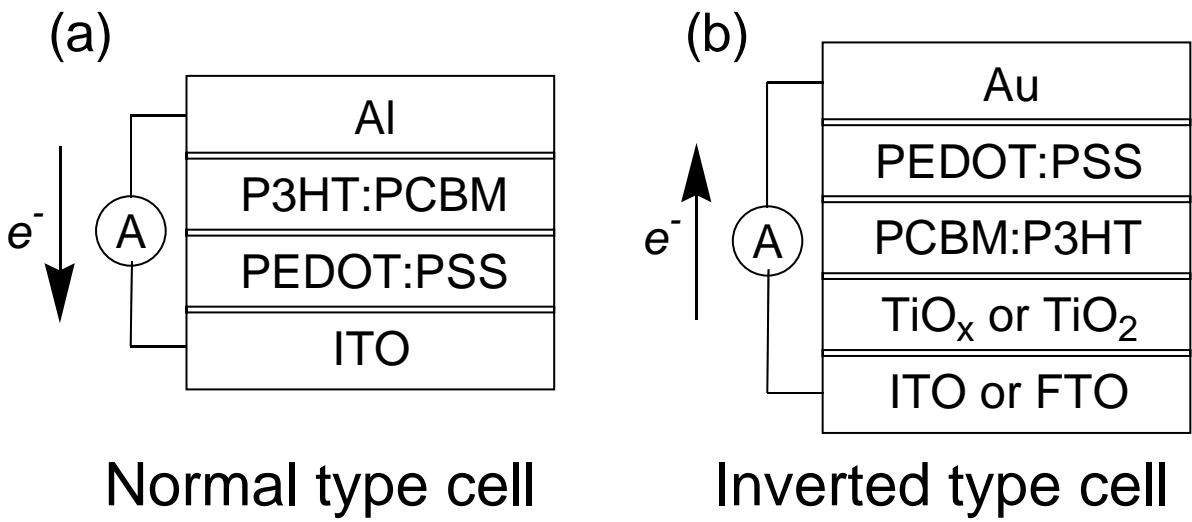
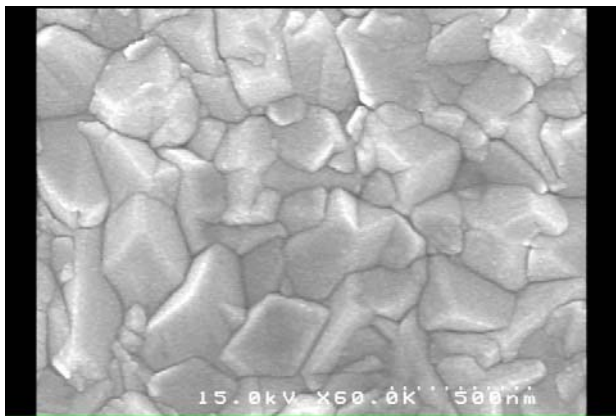


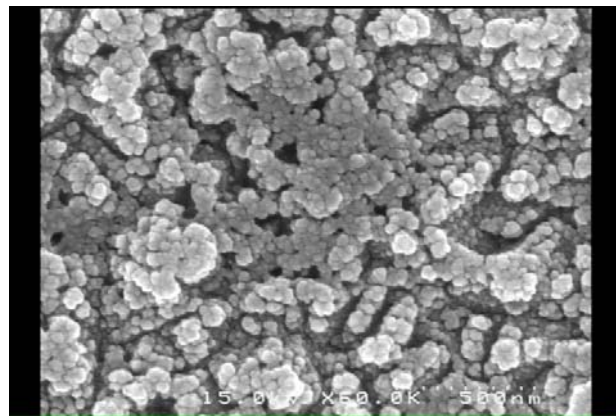
Figure 1

Kuwabara et al.

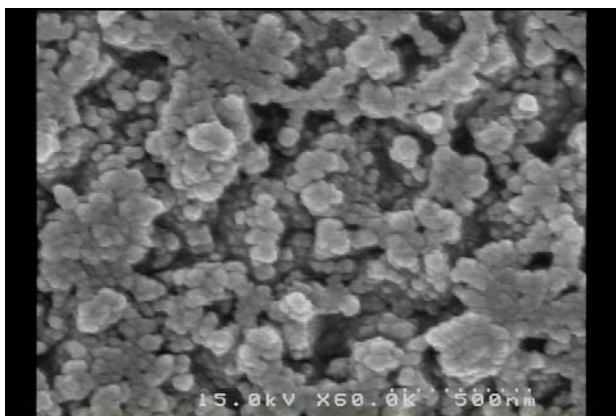
(a)



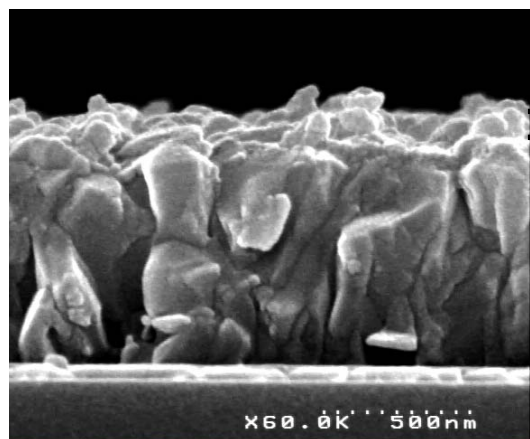
(b)



(c)



(d)



TiO<sub>2</sub> zone  
↓  
FTO

(e)

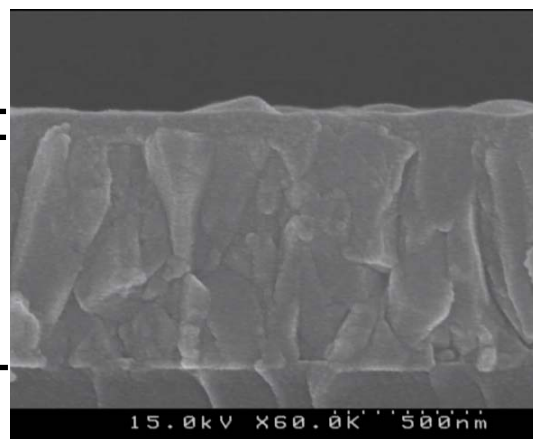


Figure 2  
Kuwabara et al.

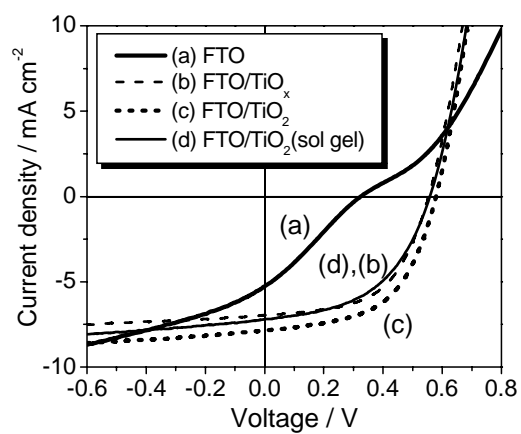


Figure 3

Kuwabara et al.

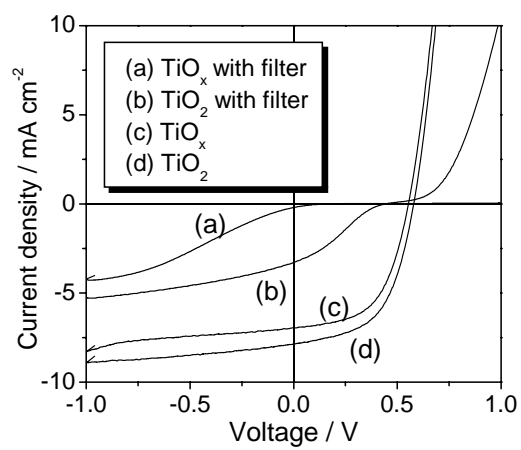


Figure 4

Kuwabara et al.

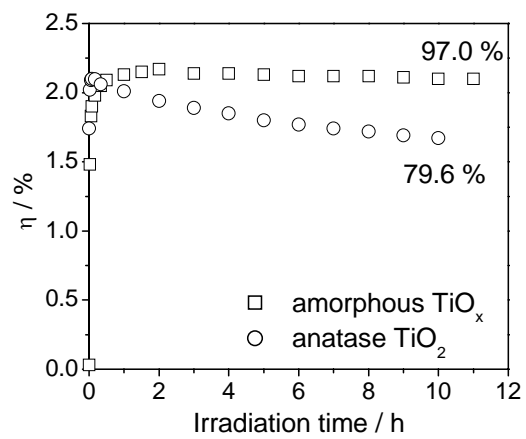


Figure 5

Kuwabara et al.